Journal of Quantitative Spectroscopy & Radiative Transfer 236 (2019) 106593

Contents lists available at ScienceDirect

Journal of Quantitative Spectroscopy & Radiative Transfer

journal homepage: www.elsevier.com/locate/jqsrt

First high–resolution analysis of the $2\nu_1(A_1)$ and $\nu_1+\nu_3(F_2)$ interacting states of $^{72}GeH_4$ and $^{73}GeH_4$

O.N. Ulenikov[a,*], O.V. Gromova[a], E.S. Bekhtereva[a], N.I. Raspopova[a], M.A. Koshelev[b], I.A. Velmuzhova[c], P.G. Sennikov[c], A.D. Bulanov[c], A.V. Kuznetsov[d], C. Leroy[d]

[a] Research School of High–Energy Physics, National Research Tomsk Polytechnic University, Tomsk 634050, Russia
[b] Institute of Applied Physics, Russian Academy of Sciences, Nizhny Novgorod 603950, Russia
[c] G.G. Devyatykh Institute of Chemistry of High Purity Substances, Russian Academy of Sciences, Nizhny Novgorod 603950, Russia
[d] Laboratoire Interdisciplinaire Carnot de Bourgogne, UMR CNRS 6303, Université Bourgogne Franche-Comté, Dijon Cedex 21078, France

ARTICLE INFO

Article history:
Received 8 July 2019
Revised 30 July 2019
Accepted 30 July 2019
Available online 31 July 2019

Keywords:
The $2\nu_1/\nu_1+\nu_3$ interacting states of GeH_4
Resonance interactions in spherical top molecules
Determination of spectroscopic parameters

ABSTRACT

The spectra of germane $^{72}GeH_4$ and $^{73}GeH_4$ enriched up to 99.9 % were recorded with high resolution (0.003 cm^{-1}) at different pressures with the Bruker IFS 125HR Fourier transform spectrometer (Nizhny Novgorod, Russia). The region of 4020–4260 cm^{-1}, where the $2\nu_1(A_1)$ and $\nu_1+\nu_3(F_2)$ bands are located, was theoretically analyzed. The 2025 and 1774 transitions with $J^{max}=21$ were assigned to these bands of the $^{72}GeH_4$ and $^{73}GeH_4$ species. Rotational, centrifugal distortion, tetrahedral splitting, and interaction parameters of the (2000, A_1) and (1010, F_2) vibrational states were determined from the fit of experimental line positions of both isotopologues. The obtained sets of 13/13 fitted parameters reproduce the initial 2025/1774 experimental line positions with a $d_{rms}=2.9\times10^{-4}$ cm^{-1} and $d_{rms}=2.7\times10^{-4}$ cm^{-1} (for $^{72}GeH_4$ and $^{73}GeH_4$, respectively).

1. Introduction

In recent papers (see [1–4] and references cited therein) we presented results of analysis of high–resolution spectra of $^{72}GeH_4$, $^{73}GeH_4$, $^{74}GeH_4$, and $^{76}GeH_4$ which have been enriched up to 88.1–99.9 % of abundance of separate species in a sample in the region of the first Dyad and Pentad. Analogously, spectra of the $^{74}GeH_4$ and $^{76}GeH_4$ species were analyzed in the region of location of the $2\nu_1(A_1)$ and $\nu_1+\nu_3(F_2)$ bands, [5]. In the present study we focus on the $2\nu_1(A_1)$ and $\nu_1+\nu_3(F_2)$ bands of $^{72}GeH_4$ and $^{73}GeH_4$ isotopologues which have been enriched up to the abundance of 99.9 % each in two different samples.

Earlier high resolution spectra of germane, an important molecule for numerous both pure academical and applied problems of astrophysics, study of atmospheres of giant gas–planets, industry, etc. (e.g., [6–15]), have been discussed in a number of papers (see, e.g., [16–38]). As to the $2\nu_1(A_1)$ and $\nu_1+\nu_3(F_2)$ bands, they have been experimentally studied in [39] (Perkin–Elmer 225 Grating Infrared Spectrophotometer; moderately high resolution of 0.040–0.045 cm^{-1}), [40] (resolution of 0.015–0.025 cm^{-1}), and [41] (FT; resolution of 0.01 cm^{-1}). In the latter study [41], transition with $J^{max}\leq8$ have been assigned to the $2\nu_1(A_1)$ and $\nu_1+\nu_3(F_2)$ bands and used in the fit with the Hamiltonian model from Refs. [42–46]. The $2\nu_1(A_1)$ and $\nu_1+\nu_3(F_2)$ bands of $^{76}GeH_4$ (88.1% in the sample) and $^{74}GeH_4$ (11.5% in the sample) have been analyzed recently with a resolution of 0.003 cm^{-1}) in Ref. [5]. In the present study two spectra of $^{72}GeH_4$ and two spectra of $^{73}GeH_4$ (both enriched up to 99.9 %) were recorded at different pressures with a resolution of 0.003 cm^{-1} and ro–vibrational transitions were assigned up to $J^{max}=21$.

2. Experimental details

Two samples of germane containing 99.9% of the $^{72}GeH_4$ and $^{73}GeH_4$ isotopologues were used in the present study. A method of the sample preparation is similar to that described in [5]. Briefly, samples of germane in natural abundance were synthesized at the Institute of Chemistry of High–Purity Substances of the Russian Academy of Sciences in Nizhny Novgorod by a reaction between $GeCl_4$ and sodium borohydride with subsequent purification by the rectification method. Then samples were enriched with the ^{72}Ge and ^{73}Ge isotopes using the centrifugal method at the Joint Stock Company Production Association Electrochemical Plant, Zelenogorsk, Russia. The enriched samples were repeatedly purified by the rectification method.

* Corresponding author.
E-mail address: ulenikov@mail.ru (O.N. Ulenikov).

https://doi.org/10.1016/j.jqsrt.2019.106593
0022-4073/

Table 1
Experimental setup for the regions 1900 - 4400 cm^{-1} of the infrared spectra of $^{M}GeH_4$ ($M = 72, 73$).

Spectrum	Substance	Resolution /cm^{-1}	Measuring time/h	No. of scans	Source	Detector	Beam-splitter	Opt. path-length/m	Aperture /mm	Temp. /°C	Pressure /Torr
I	$72GeH_4$	0.003	35.2	1050	Globar	InSb	KBr	3.75	1.15	24.5	0.4
II	$72GeH_4$	0.003	41.9	1250	Globar	InSb	KBr	3.75	1.15	24.2	4.0
III	$73GeH_4$	0.003	33.5	1000	Globar	InSb	KBr	3.75	1.0	24.9	0.4
IV	$73GeH_4$	0.003	33.5	1000	Globar	InSb	KBr	3.75	1.0	25.3	3.0

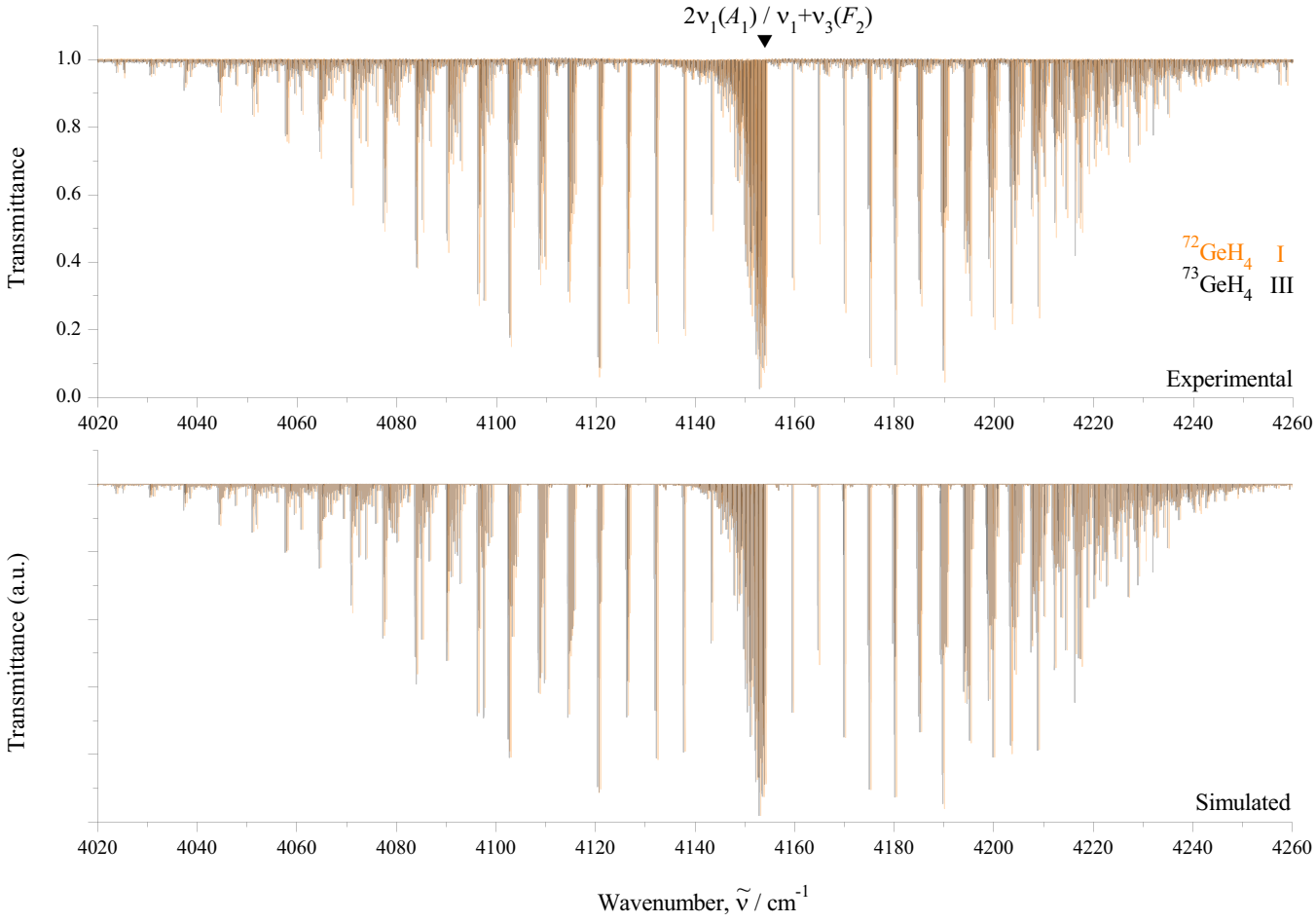

Fig. 1. Survey spectra I (orange) and III (black) of $^{72}GeH_4$ and $^{73}GeH_4$ enriched up to 99.9 % (upper trace) in the region of 4020–4260 cm^{-1} (for the experimental conditions, see Table 1). The bottom traces present corresponding simulated spectra. (For interpretation of the references to colour in this figure legend, the reader is referred to the web version of this article.)

Spectra of the gas sample of germane were recorded using a Bruker IFS125HR Fourier transform spectrometer. The experimental details are presented in Table 1. Briefly, the spectrometer was equipped with a Globar source, a KBr beam splitter and indium antimonide (InSb) detectors. The spectra were recorded with a resolution of 0.003 cm^{-1} (the resolution due to the maximum optical path difference) in the frequency range of 1900–4400 cm^{-1} (in this paper spectra are discussed in the region of 4020–4260 cm^{-1}). The Norton–Beer (weak) apodization function was applied. To study both strong and weak lines, spectra were recorded at different pressures; a multi–pass White cell was used. A cell was permanently connected to a gas sample vacuum system, a turbo–molecular pump, and capacitance pressure gauges covering the 10^{-3} – 100 Torr range. The optical compartment of the spectrometer was pumped out by a mechanical pump down to 0.02 Torr (or less) and that pressure remained constant during the experiments.

The final spectra (see Figs. 1–3) were obtained by averaging 1000–1250 scans. In total, two spectra of $^{72}GeH_4$ and two spectra of $^{73}GeH_4$ were recorded. Spectra were calibrated using the most intense and well resolved H_2O (more than 80 lines) and CO_2 (more than 50 lines) lines from the HITRAN database line list [47]. After calibration the standard deviation of the difference between the measured and tabulated peak positions was estimated to be less than 3×10^{-4} cm^{-1}.

3. Brief theoretical background

Germane is a spherical top molecule which symmetry group is isomorphic to the T_d point symmetry group. This molecule has a tetrahedral structure resulting in one nondegenerate (q_1, A_1), one doubly degenerate (q_2, E), and two triply degenerate (q_3, F_2) and (q_4, F_2) vibrational modes. It is well known (see, e.g., Refs. [48–50]) that ro–vibrational states of such molecules are

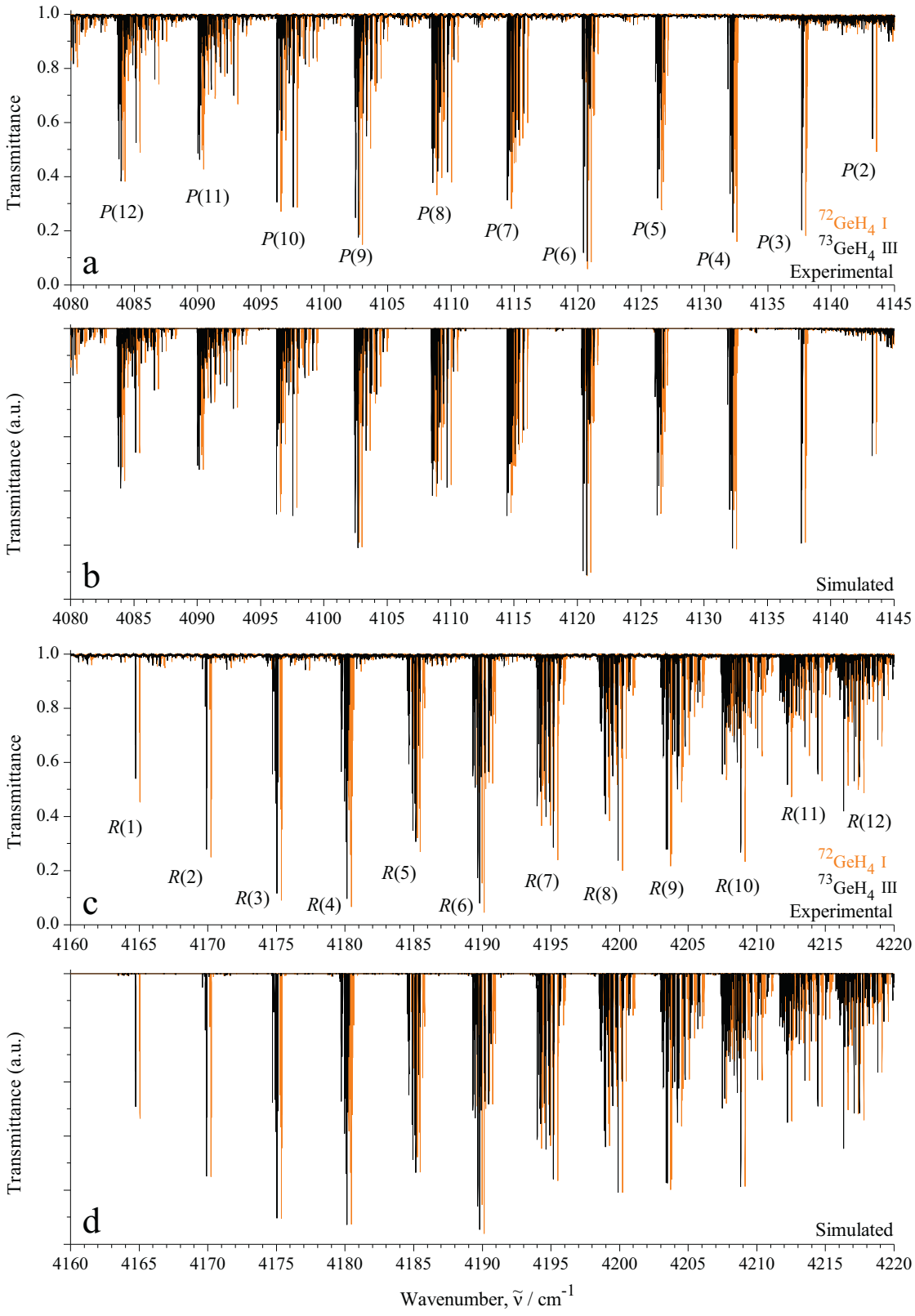

Fig. 2. Experimental spectra of $^{72}GeH_4$ and $^{73}GeH_4$ in the region of the *P*–branch (Fig. 2a) and (the *R*–branch (Fig. 2c); for the experimental conditions, see Table 1. The traces 2b and 2d present corresponding simulated spectra.

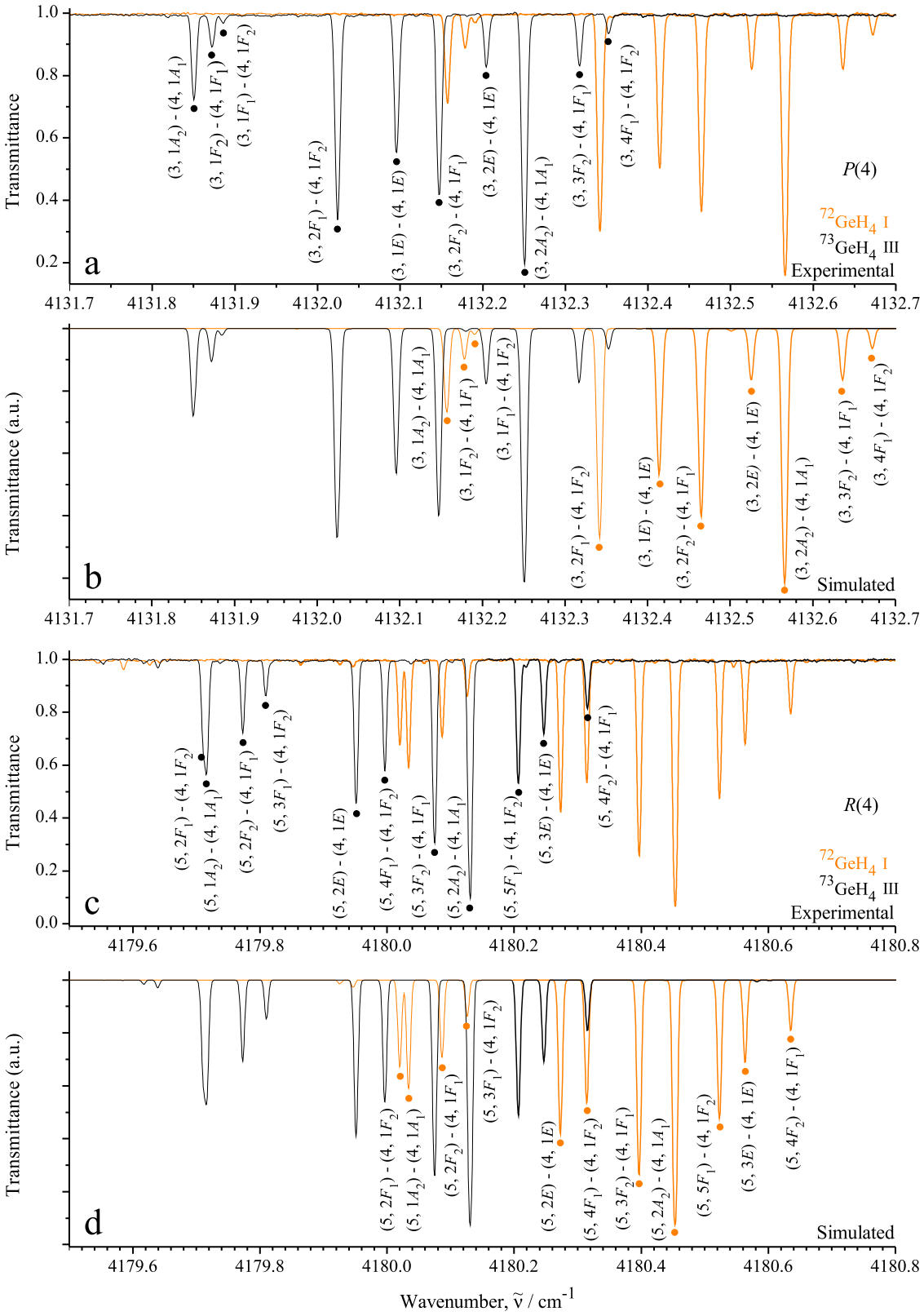

Fig. 3. Small portions (traces 3a and 3c) of the high–resolution experimental spectra I and III of $^{72}GeH_4$ and $^{73}GeH_4$ in the region of the $P(4)$ and $R(4)$ clusters of the $2\nu_1(A_1)/\nu_1 + \nu_3(F_2)$ bands. For the experimental conditions, see Table 1. The traces 3b and 3d present corresponding simulated spectra.

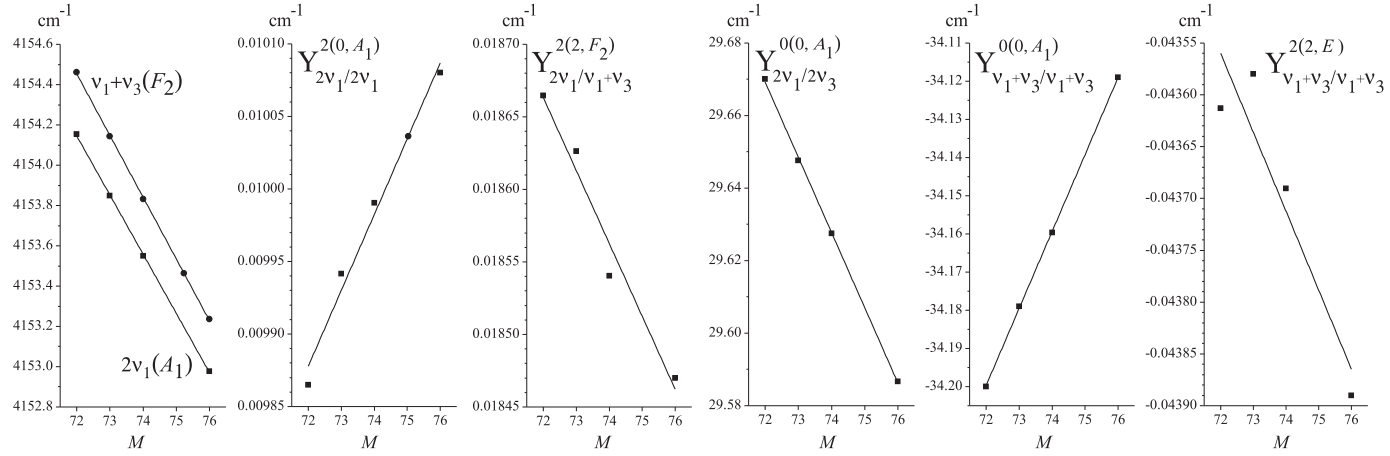

Fig. 4. Plots of dependence of the values (in cm^{-1}) of some spectroscopic parameters of $^{M}GeH_4$ on the mass M of the ^{M}Ge nucleus (experimental data are taken from this study and from [5]).

divided into groups (polyads) of more or less isolated states which interact with each other inside of a polyad. In the present paper we deal with a pair of stretching bands $2\nu_1(A_1)$ and $\nu_1+\nu_3(F_2)$ which belong to the so–called tetradecad vibrational region. As the analysis shows, interaction of these two bands with the pure bending and/or stretching–bending bands of the tetradecad can be neglected for germane. At the same case, it is necessary to take into account (see, e.g., [5]) strong interaction of the $2\nu_1(A_1)$ and $\nu_1+\nu_3(F_2)$ bands with the third stretching band of the tetradecad, namely, $2\nu_3$ which consists of three sub–bands, $2\nu_3(F_2)$, $2\nu_3(E)$ and $2\nu_3(A_1)$. The latter three sub–bands, which are located near $4220\,cm^{-1}$, are very weak and are not seen in the spectra, see Figs. 1 and 3 (weakness of the $2\nu_3$ band is explained by the local mode theory, [51–57] as a borrowing of intensity by the $2\nu_1(A_1)/\nu_1+\nu_3(F_2)$ bands from $2\nu_3$ because of strong resonance interaction between all of them.

The high symmetry of the GeH_4 molecule requires using a special mathematical formalism: the theory of Irreducible Tensorial Sets (see, e.g., Refs. [58–61]) for the description of its spectra. Application of the mentioned formalism to the XY_4 (T_d) molecules has been discussed in the spectroscopic literature many times (see, e.g., Refs. [62–66]). For that reason we present only briefly the main points necessary for understanding the procedure of calculations with the effective Hamiltonian of the XY_4 spherical top molecule.

As is known from general vibration-rotation theory [67–69], the Hamiltonian of an arbitrary polyatomic molecule can be reduced to a set of the so–called effective Hamiltonians, or, in a more general case, to a set of effective operator matrices of the form (it was discussed in the literature many times, see, e.g., [70–72])

$$H^{vib.-rot.} = \sum_{a,b} |a\rangle\langle b| H^{a,b}, \tag{1}$$

where $|a\rangle$ and $\langle b|$ are the basic vibrational functions; the operators $H^{a,b}$ depend on the rotational operators J_α ($\alpha = x, y, z$) only, and summation is performed on all degenerate and/or interacting vibrational states. When, as in our case, a molecule possesses a symmetry, Eq. (1) can be rewritten in the symmetrized form [61]:

$$\begin{aligned} H^{vib.-rot.} &= \sum_{\nu\gamma,\nu'\gamma'} \sum_{n\Gamma} [(|\nu\gamma\rangle \otimes \langle\nu'\gamma'|)^{n\Gamma} \otimes H^{n\Gamma}_{\nu\gamma,\nu'\gamma'}]^{A_1} \\ &\equiv \sum_{\nu\gamma,\nu'\gamma'} \sum_{n\Gamma} \sum_{\Omega K} \left[(|\nu\gamma\rangle \otimes \langle\nu'\gamma'|)^{n\Gamma} \otimes R^{\Omega(K,n\Gamma)}\right]^{A_1} Y^{\Omega(K,n\Gamma)}_{\nu\gamma,\nu'\gamma'}. \end{aligned} \tag{2}$$

In Eq. (2):

(a) $|\nu\gamma\rangle$ are the symmetrized vibrational functions, γ are symmetries of these functions; $R^{\Omega(K,n\Gamma)}_\sigma$ are symmetrized rotational operators, and Ω is the total degree of the rotational operators J_α in the individual operator R; K is the rank of this operator (see, e.g., [73]), Γ is its symmetry in the T_d point symmetry group, and n distinguishes between different possible operators $R^{\Omega(K,n\Gamma)}_\sigma$ having the same values of Ω, K and Γ. The sign $\otimes$ denotes a tensorial product, and the values $Y^{\Omega(K,n\Gamma)}_{\nu\gamma,\nu'\gamma'}$ are different–type spectroscopic parameters.

(b) The symmetrized rotational operators, $R^{\Omega(K,n\Gamma)}_\sigma$, are determined as, [73]),

$$R^{\Omega(K,n\Gamma)}_\sigma = \sum_m {}^{(K)}G^m_{n\Gamma\sigma} R^{\Omega(K)}_m, \tag{3}$$

where the rotational operators $R^{\Omega(K)}_m$ are symmetrized in the SO(3) symmetry group and can be constructed in accordance with the recurrence relation, [66,73]:

$$R^{\Omega+1(K+1)}_{\tilde m} = \sum_{l=-1,0,1} C^{K+1\ \tilde m}_{K\ \tilde m-l,1\ l} R^{\Omega(K)}_{\tilde m-l} R^{1(1)}_l, \tag{4}$$

where $C^{K+1\ \tilde m}_{K\ \tilde m-l,1\ l}$ are known Clebsh–Gordan coefficients, Ref. [60]. The irreducible rotational operators $R^{\Omega(K)}_m$ with $K<\Omega$ (in this case, the parity of both Ω and K must be the same, [73]) are constructed as,

$$R^{\Omega(K)}_m = R^{\Omega=K(K)}_m (R^{2(0)})^{(\Omega-K)/2}, \tag{5}$$

where the notation $R^{2(0)} = (J^2_x + J^2_y + J^2_z)$ is used. In this case, the tensorial components of the first order operator $R^{1(1)}_m$ ($m = 0, \pm1$) are determined as

$$\begin{aligned} R^{1(1)}_1 &= -\frac{1}{\sqrt{2}}(J_x - iJ_y) \equiv -J_+, \\ R^{1(1)}_{-1} &= \frac{1}{\sqrt{2}}(J_x + iJ_y) \equiv J_-, \\ R^{1(1)}_0 &= J_z \equiv J_0, \end{aligned} \tag{6}$$

where

$$\begin{aligned} J_x &= i\frac{\cos\varphi}{\sin\theta}\left(\frac{\partial}{\partial\psi} - \cos\theta\frac{\partial}{\partial\varphi}\right) - i\sin\varphi\frac{\partial}{\partial\theta}, \\ J_y &= -i\frac{\sin\varphi}{\sin\theta}\left(\frac{\partial}{\partial\psi} - \cos\theta\frac{\partial}{\partial\varphi}\right) - i\cos\varphi\frac{\partial}{\partial\theta}, \end{aligned} \tag{7}$$

and

$$J_z = -i\frac{\partial}{\partial\varphi}. \tag{8}$$

The values ${}^{(K)}G^m_{n\Gamma\sigma}$ in Eq. (3) are so–called reduced matrix elements, which can be found in the literature (see, e.g., [63,74,75]).

Table 2
Statistical information for the $2\nu_1/\nu_1+\nu_3$ local mode bands of $^{72}GeH_4$ and $^{73}GeH_4$.

Band	Center/cm^{-1}		J^{max}	N_t[a]	N_p[b]	m_1[c]	m_2[c]	m_3[c]
	pw[d]	Ref.[79][e]						
1	2	3	4	5	6	7	8	9
		$^{72}GeH_4$						
$\nu_1+\nu_3(F_2)$	4154.46177	4154.468						
			21	2025	13	56.4	27.2	16.4
$2\nu_1(A_1)$	4154.15275	4154.154						
d_{rms}	2.9×10^{-4}cm^{-1}							
		$^{73}GeH_4$						
$\nu_1+\nu_3(F_2)$	4154.14255	4154.142						
			21	1774	13	62.4	25.1	12.5
$2\nu_1(A_1)$	4153.84762	4153.847						
d_{rms}	2.7×10^{-4}cm^{-1}							

[a] N_t is the number of transitions.
[b] N_p is the number of fitted parameters.
[c] Here $m_i = n_i/N\times100\%$ (i = 1, 2, 3); n_1, n_2, and n_3 are the numbers of transitions for which the differences $\delta = E^{exp}-E^{calc}$ ($\delta = \nu^{exp}-\nu^{calc}$) satisfy the conditions $\delta\le2\times10^{-4}$ cm^{-1}, 2×10^{-4} cm^{-1} $<\delta\le4\times10^{-4}$ cm^{-1}, and $\delta>4\times10^{-4}$ cm^{-1}.
[d] Obtained from the fit in the present work.
[e] Reproduced, for comparison, from Ref. [79].

4. Description of the spectra and assignment of transitions

The upper part of Fig. 1 presents the survey spectra I (orange) and III (black) of $^{72}GeH_4$ and $^{73}GeH_4$ in the region of 4020–4260 cm^{-1}. One can see clearly pronounced all three branches of the $2\nu_1(A_1)/\nu_1+\nu_3(F_2)$ local mode bands and minor shifts of the lines belonging to the $^{73}GeH_4$ isotopologue relatively the lines belonging to the $^{72}GeH_4$ isotopologue. For the illustration, two smaller parts of spectra are shown in Fig. 2a (clusters $P(2)-P(12)$ of the $P-$branch) and Fig. 2c (clusters $R(1)-R(12)$ of the $R-$branch). Figs. 3a and c present small fragments of the high–resolution spectra of clusters $P(4)$ and $R(4)$. Figs. 3c and d demon-

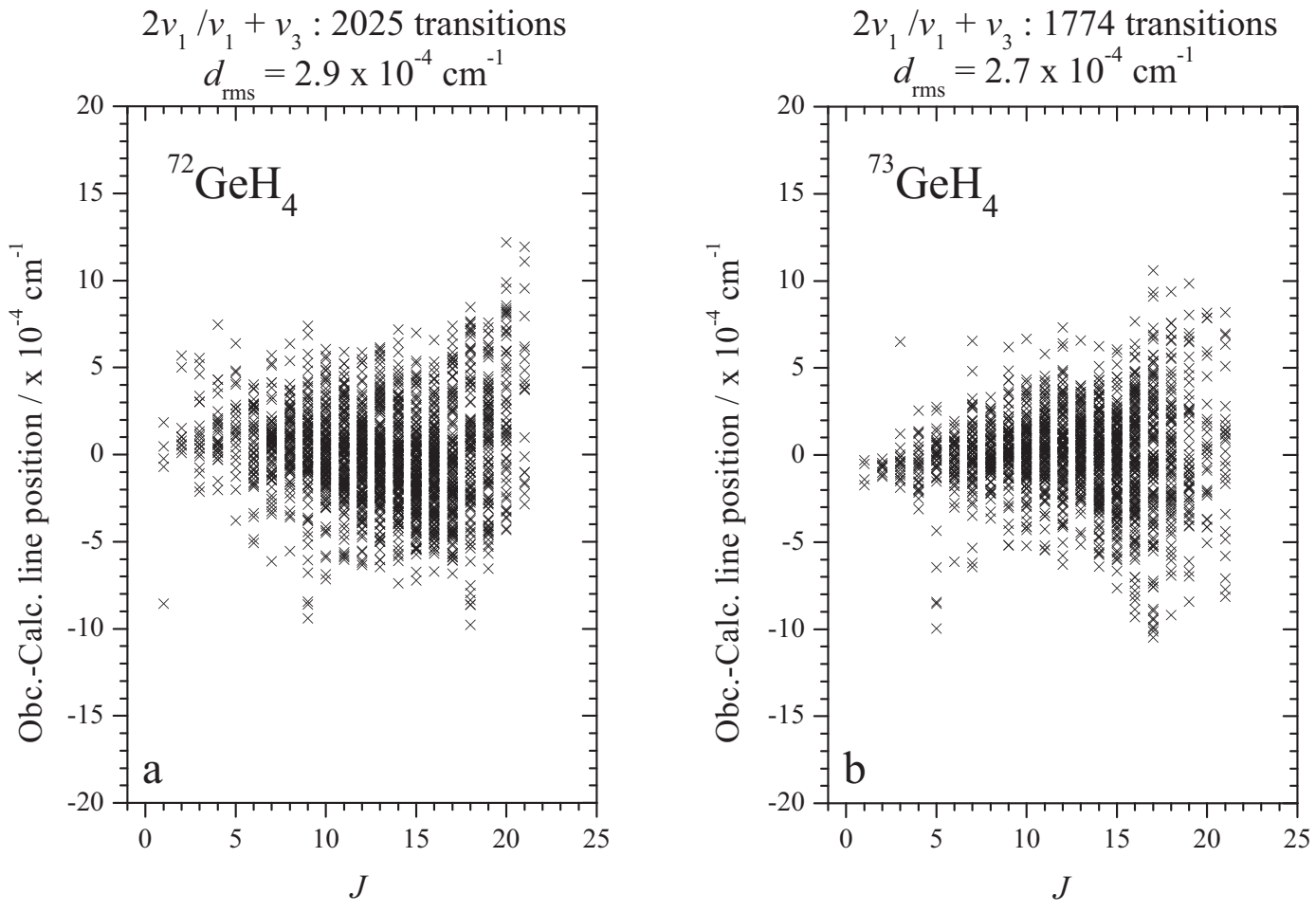

Fig. 5. Observed – calculated line positions and fit statistics for bands studied in the present paper: Fig. 5a and b correspond to the $\nu_1+\nu_3(F_2)/2\nu_1(A_1)$ bands of $^{72}GeH_4$ and $^{73}GeH_4$, respectively.

Table 3
Spectroscopic parameters $Y^{\Omega(K,n\Gamma)}_{v\gamma,v'\gamma'}$ of the stretching bands of tetradecad of Germane (in cm^{-1})[a].

(v, γ)	(v', γ')	$\Omega(K, n\Gamma)$	$^{72}GeH_4$[b]	$^{73}GeH_4$[b]	$^{74}GeH_4$[c]	$^{76}GeH_4$[c]
1	2	3	4	5	6	7
(2000, A_1)	(2000, A_1)	0(0, A_1)	-17.18	-17.165	-17.15	-17.12
	(2000, A_1)	2(0, A_1)	0.00986495(29)	0.00994156(34)	0.00999042(64)	0.01008(87)
	(2000, A_1)	4(0, A_1)10^5	0.1793	0.1793	0.1793	0.1793(58)
	(2000, A_1)	4(4, A_1)10^6	−0.4370	−0.4370	−0.4370	−0.4370(89)
(2000, A_1)	(1010, F_2)	2(2, F_2)	0.018664602(76)	0.018626372(18)	0.0185404(18)	0.01847(18)
	(1010, F_2)	3(3, F_2)10^5	0.8730	0.86193(47)	0.835	0.835(74)
	(1010, F_2)	4(4, F_2)10^5	0.2389	0.2389	0.2389	0.2389(19)
(2000, A_1)	(0020, A_1)	0(0, A_1)	29.67	29.647641(15)	29.627518(26)	29.586665(25)
	(0020, A_1)	2(0, A_1)10^2	0.338	0.334	0.334	0.334(25)
(1010, F_2)	(1010, F_2)	0(0, A_1)	-34.20	-34.179018(10)	-34.159643(13)	-34.118998(18)
	(1010, F_2)	1(1, F_1)	−0.388	−0.3900425(43)	−0.3921452(29)	−0.396(18)
	(1010, F_2)	2(0, A_1)	0.022259913(68)	0.022185227(64)	0.02225060(23)	0.02237(35)
	(1010, F_2)	2(2, E)	−0.04361287(10)	−0.043579816(98)	−0.04369038(31)	−0.04389(41)
	(1010, F_2)	2(2, F_2)	−0.0199680(18)	−0.01977	−0.01973	−0.01973(32)
	(1010, F_2)	3(1, F_1)10^3	0.1672230(71)	0.1675280(80)	0.1675	0.1675(39)
	(1010, F_2)	3(3, F_1)10^3	0.2130077(60)	0.2136394(46)	0.2158	0.2158(31)
	(1010, F_2)	4(0, A_1)10^5	0.1210	0.1210	0.1210	0.1210(22)
	(1010, F_2)	4(2, E)10^6	0.521	0.521	0.521	0.521(13)
	(1010, F_2)	4(2, F_2)10^7	−0.3262(25)	−0.2258(26)	0.0	0.0
	(1010, F_2)	4(4, E)10^6	0.39405(17)	0.40734(20)	0.428	0.428(18)
(1010, F_2)	(0020, A_1)	2(2, F_2)	−0.01609	−0.01609	−0.01609	−0.01609(11)
(1010, F_2)	(0020, E)	1(1, F_1)	-3.290	-3.290	-3.290	-3.290(31)
	(0020, E)	2(2, F_2)10^2	0.688	0.688	0.688	0.688(31)
(1010, F_2)	(0020, F_2)	0(0, A_1)	-34.865933(86)	-34.10	-34.10	-34.10
	(0020, F_2)	1(1, F_1)	0.1756	0.1756	0.1756	0.1756(88)
	(0020, F_2)	2(0, A_1)10^2	−0.6665	−0.6665	−0.6665	−0.6665(98)
	(0020, F_2)	2(2, E)	0.01612	0.01612	0.01612	0.01612(31)
	(0020, F_2)	2(2, F_2)10^3	0.16230(88)	0.0	0.0	0.0
(0020, A_1)	(0020, A_1)	0(0, A_1)	-50.976888(15)	-51.42	-51.42	-51.42
(0020, E)	(0020, E)	0(0, A_1)	0.0	0.0	0.0	0.0
	(0020, E)	2(0, A_1)10^2	−0.303	−0.303	−0.303	−0.303(14)
	(0020, E)	2(2, E)10^2	−0.925	−0.925	−0.925	−0.925(16)
(0020, E)	(0020, F_2)	1(1, F_1)	1.994	1.993	1.991894(19)	1.990(42)
(0020, F_2)	(0020, F_2)	0(0, A_1)	-33.90603(18)	-34.10	-34.10	-34.10
	(0020, F_2)	2(2, F_2)	−0.01629	−0.01632243(18)	−0.01636	−0.01636(30)

[a] Values in parentheses are 1σ statistical confidence intervals. Parameters of $^{72}GeH_4$/$^{73}GeH_4$ presented without confidence intervals were constrained to the values of corresponding parameters of the $^{76}GeH_4$/$^{74}GeH_4$ isotopologues, or estimated from interpolation/extrapolation of corresponding values of other isotopologues and were not varied in the fit.
[b] This work.
[c] Reproduced, for comparison, from Ref. [5].

strate that, in spite of the fact of only minor change at the transition from the $^{72}GeH_4$ molecule to the $^{73}GeH_4$ one, even qualitative differences can be seen in their high–resolution spectra. In particular, one can see from these figures that the $(5, 2F_1) - (4, 1F_2)$ and $(5, 1A_2) - (4, 1A_1)$ transitions of the $^{73}GeH_4$ isotopologue look like one line, but the same transitions for the $^{72}GeH_4$ look already like two separate lines.

As was mentioned above, the GeH_4 molecule is a spherical top with a symmetry group isomorphic to the T_d point symmetry group. As a consequence, transitions in absorption are allowed only between vibrational states $(v\Gamma)$ and $(v'\Gamma')$ for which the relation (see, *e.g.*, [76,77])

$$\Gamma \otimes \Gamma' \ni F_2 \tag{9}$$

is fulfilled. As a consequence, the $\nu_1 + \nu_3(F_2)$ band is allowed, but the $2\nu_1(A_1)$ band appears in absorption only because of strong Coriolis interaction with the $\nu_1 + \nu_3(F_2)$ one.

For assignment of transitions we used information about the ro–vibrational structure of the $2\nu_1(A_1)/\nu_1 + \nu_3(F_2)$ bands of the $^{76}GeH_4$ and $^{74}GeH_4$ species from Ref. [5]. In this case, following the results and statements of the isotopic substitution theory, [78], knowledge of positions of lines of the same name of $^{76}GeH_4$ and $^{74}GeH_4$ gave us possibility to predict without doubt and with a high accuracy positions of corresponding lines for the $^{73}GeH_4$ and $^{72}GeH_4$ isotopologues ($J^{max} = 7$). Assignment of transitions with higher values of quantum number J was fulfilled simultaneously with the fit of spectroscopic parameters of the effective Hamiltonian, Eq. (2). Finally, 2025 and 1774 transitions with the maximum value of upper quantum number $J^{max} = 21$ were assigned to the $\nu_1 + \nu_3(F_2)/2\nu_1(A_1)$ bands of the $^{72}GeH_4$ and $^{73}GeH_4$ isotopologues. The obtained data is a considerable extension of the before known information about spectroscopic properties of $^{72}GeH_4$ and $^{73}GeH_4$ (compare, e.g., with the later study, Ref. [41]; see also statistical information in Table 2). The list of assigned transitions is presented in the Supplementary material. It is necessary to mark that, because of the local mode behavior of the $\nu_1 + \nu_3(F_2)/2\nu_1(A_1)$ bands, it is difficult to distinguish between lines of the $\nu_1 + \nu_3(F_2)$ and $2\nu_1(A_1)$ bands. For this reason, to distinguish between transitions of the same symmetry in a concrete cluster (the same as in the Dijon XTDS notation, [80]) we used numbers $n = 1, 2, 3, ...$ In this case, increase of the wavenumber of transition corresponds to increase of the number n.

5. Ro–vibrational analysis and parameters of the effective Hamiltonian

All the 3799 experimental transitions discussed in the before section were used as the initial information in the weighted fit procedure to determine the parameters of the effective Hamiltonian given by Eq. (2). Values of spectroscopic parameters of the $^{74}GeH_4$ isotopologue were taken as the initial values both for the $^{73}GeH_4$ and $^{72}GeH_4$ species. Such approach is suitable enough because mass of ^{M}Ge nucleus is barely changed under isotopic substitution. The values of parameters obtained from the

Table 4
Spectroscopic parameters $Y^{\Omega(K,n\Gamma)}_{\nu\gamma,\nu'\gamma'}$ of the (0000, A_1), (1000, A_1), and (0010, F_2) vibrational states of germane.

(ν, γ)	(ν', γ')	$\Omega(K, n\Gamma)$	$^{72}GeH_4$[a]	$^{73}GeH_4$[b]	$^{74}GeH_4$[c]	$^{76}GeH_4$[c]
1	2	3	4	5	6	7
(0000, A_1)	(0000, A_1)	2(0, A_1)	2.695859440	2.69586298	2.695864734	2.695870305
	(0000, A_1)	4(0, A_1)10^4	−0.3341682	−0.3341682	−0.3341682	−0.3341682
	(0000, A_1)	4(4, A_1)10^5	−0.1547079	−0.1547079	−0.1547079	−0.1547079
	(0000, A_1)	6(0, A_1)10^8	0.114368	0.114368	0.114368	0.114368
	(0000, A_1)	6(4, A_1)10^{10}	−0.51075	−0.51075	−0.51075	−0.51075
	(0000, A_1)	6(6, A_1)10^{10}	−0.15638	−0.15638	−0.15638	−0.15638
(1000, A_1)	(1000, A_1)	0(0, A_1)	2110.7088020	2110.7042698	2110.7004560	2110.691769
	(1000, A_1)	2(0, A_1)10^2	−1.7988113	−1.7988113	−1.799331	−1.799331
	(1000, A_1)	4(0, A_1)10^6	0.17727	0.17727	−0.19367	−0.19367
	(1000, A_1)	4(4, A_1)10^8	−0.4386	−0.4386	−0.420	−0.420
(1000, A_1)	(0010, F_2)	2(2, F_2)10^2	−0.8100331	−0.8095009	−0.8091897	−0.8076987
	(0010, F_2)	3(3, F_2)10^5	−0.175232	−0.170815	−0.14853	−0.14853
	(0010, F_2)	4(2, F_2)10^6	−0.111586	−0.111586	−0.10836	−0.10836
	(0010, F_2)	4(4, F_2)10^6	−0.158576	−0.158576	−0.15996	−0.15996
	(0010, F_2)	5(5, F_2)10^9	0.2873	0.2873	0.2873	0.2873
(0010, F_2)	(0010, F_2)	0(0, A_1)	2111.5739400	2111.3545845	2111.1420507	2110.7323088
	(0010, F_2)	1(1, F_1)	−0.55568226	−0.55907227	−0.56236859	−0.5686669
	(0010, F_2)	2(0, A_1)	−0.0147050657	−0.014700452	−0.014695020	−0.01468601
	(0010, F_2)	2(2, E)10^2	0.2275549	0.2263509	0.2254772	0.2234550
	(0010, F_2)	2(2, F_2)10^2	−0.4470184	−0.4472682	−0.447832	−0.447832
	(0010, F_2)	3(1, F_1)10^5	−0.745775	−0.75253	0.76349	−0.76349
	(0010, F_2)	3(3, F_1)10^5	−0.65737	−0.65737	−0.64671	−0.64671
	(0010, F_2)	4(0, A_1)10^8	0.3970	0.3970	0.0	0.0
	(0010, F_2)	4(2, E)10^7	0.93688	0.91672	0.9537	0.9537
	(0010, F_2)	4(2, F_2)10^7	−0.6775	−0.6775	−0.6775	−0.6775
	(0010, F_2)	4(4, A_1)10^7	0.10694	0.10694	0.10694	0.10694
	(0010, F_2)	4(4, E)10^7	0.1407	0.1407	0.1407	0.1407
	(0010, F_2)	4(4, F_2)10^6	−0.20740	−0.20740	−0.20740	−0.20740
	(0010, F_2)	5(1, F_1)10^9	−0.558	−0.558	−0.558	−0.558
	(0010, F_2)	5(3, F_1)10^9	−0.18787	−0.18787	0.0	0.0
	(0010, $1F_2$)	5(5, F_1)10^9	0.34126	0.34126	0.370	0.370
	(0010, $3F_2$)	5(5, F_1)10^9	−0.66037	−0.66037	−0.639	−0.639

[a] Reproduced from [4].
[b] Reproduced from [3].
[c] Reproduced from [2].

fit are presented in columns 4 and 5 of Table 3 together with their 1σ confidence statistical intervals (the latter are given in parentheses). Parameters in Table 3, which are shown without parentheses, have been constrained to the values of corresponding parameters of the $^{76}GeH_4$/$^{74}GeH_4$ isotopologues, or estimated from interpolation/extrapolation of corresponding values of other isotopologues and were not varied in the fit. As in our recent studies of the spherical top molecules, for the convenience of the reader, in Table 3 we use the notation of parameters which corresponds to the XTDS/Dijon software, [80]. For this reason, Table 4 presents spectroscopic parameters of the ground and of the (0010, F_2)/(1000, A_1) vibrational states. Correctness of the results is confirmed by the following facts:

(1) 13 parameters, obtained from the fit, reproduce 2025 initial experimental line positions of the $\nu_1+\nu_3(F_2)/2\nu_1(A_1)$ bands of $^{72}GeH_4$ with the $d_{rms} = 2.9\times10^{-4}$ cm^{-1}; analogously, 13 parameters, obtained from the fit, reproduce 1774 initial experimental line positions of the $\nu_1+\nu_3(F_2)/2\nu_1(A_1)$ bands of $^{73}GeH_4$ with the $d_{rms} = 2.7\times10^{-4}$ cm^{-1}, which is closed to experimental uncertainty; corresponding differences are shown in column 4 of the Supplementary material, see also statistical information in Table 2;
(2) as can be seen from comparison of the values of parameters of the same name in Table 3 (see also Fig. 4), values of all fitted parameters of the same name are changed practically linearly vs the change of mass of the ^{M}Ge nucleus; this is in a total correspondence with the results and statements of the isotopic substitution theory;
(3) bottom part of Figs. 1 and 2b,d, 3b,d present the simulated spectra which were obtained with the parameters from Table 3 (the relative line strengths have been calculated with only the single main dipole moment parameter and Doppler line shape profile was used in calculations); one can see more than satisfactory correspondence between the experimental and simulated spectra;
(4) to give the reader a possibility to appreciate the quality of the results, Fig. 5 shows the fit residuals for line positions as a function of the quantum number J.

6. Conclusion

High resolution FTIR spectra of the $^{72}GeH_4$ and $^{73}GeH_4$ molecules enriched up to 99.9% of both species in samples were recorded with a Bruker IFS 125HR Fourier transform spectrometer in the tetradecad region. Ro–vibrational transitions belonging to the stretching $\nu_1+\nu_3(F_2)$ and $2\nu_1(A_1)$ bands were assigned in the experimental spectra. On that basis, 2025 and 1774 transitions with the maximum value of upper quantum number $J^{max} = 21$ were assigned to the $\nu_1+\nu_3(F_2)/2\nu_1(A_1)$ bands of the $^{72}GeH_4$ and $^{73}GeH_4$ isotopologues. The obtained data were used in a weighted fitting procedure to determine the spectroscopic parameters of the effective Hamiltonian. A set of 13/13 parameters obtained from the fit reproduced 2025/1774 initial line positions of the $\nu_1+\nu_3(F_2)/2\nu_1(A_1)$ bands with a $d_{rms} = 2.9\times10^{-4}$ cm^{-1} and $d_{rms} = 2.7\times10^{-4}$ cm^{-1} for $^{72}GeH_4$ and $^{73}GeH_4$, respectively.

Acknowledgments

The research was funded by the Tomsk Polytechnic University Competitiveness Enhancement Program, project VIU-63/2019.

Supplementary material

Supplementary material associated with this article can be found, in the online version, at doi:10.1016/j.jqsrt.2019.106593.

References

[1] Ulenikov ON, Gromova OV, Bekhtereva ES, Raspopova NI, Sennikov PG, Koshelev MA, Velmuzhova IA, Velmuzhov AP, Bulanov AD. High resolution study of $^{M}GeH_4$ (M = 76, 74) in the dyad region. J Quant Spectrosc Radiat Transfer 2014;144:11–26.

[2] Koshelev MA, Velmuzhov AP, Velmuzhova IA, Sennikov PG, Raspopova NI, Bekhtereva ES, Gromova OV, Ulenikov ON. High resolution study of strongly interacting $\nu_1(A_1)/\nu_3(F_2)$ bands of $^{M}GeH_4$ (M = 76, 74). J Quant Spectrosc Radiat Transfer 2015;164:161–74.

[3] Ulenikov ON, Gromova OV, Bekhtereva ES, Raspopova NI, Koshelev MA, Velmuzhova IA, Bulanov AD, Sennikov PG. High–resolution FTIR spectroscopic study of $^{73}GeH_4$ up to 2300 cm^{-1}. J Quant Spectrosc Radiat Transfer 2018;221:129–37.

[4] Ulenikov ON, Gromova OV, Bekhtereva ES, Raspopova NI, Kuznetsov AV, Koshelev MA, Velmuzhova IA, Sennikov PG. First high–resolution comprehensive analysis of $^{72}GeH_4$ spectra in the dyad and pentad regions. J Quant Spectrosc Radiat Transfer 2019;225:206–13.

[5] Ulenikov ON, Gromova OV, Bekhtereva ES, Raspopova NI, Sennikov PG, Koshelev MA, Velmuzhova IA, Velmuzhov AP, Adamchik SA. High resolution study of strongly interacting $2\nu_1(a_1)/\nu_1 + \nu_3(f_2)$ bands of $^{M}GeH_4$ (M = 76, 74). J Quant Spectrosc Radiat Transfer 2018;205:96–104.

[6] Fink U, Larson HP, Treffers RR. Germane in the atmosphere of jupiter. Icarus 1978;34:344–54.

[7] Kunde V, Hanel R, Maguire W, Gautier D, Baluteau JP, Marten A, Chédin A, Husson N, Scott N. The tropospheric gas composition of the north equatorial belt (NH_3, PH_3, CH_3D, GeH_4, H_2O) and the jovian D/H isotopic ratio. Astrophys J 1982;263:443–67.

[8] Drossart P, Encrenaz T, Kunde V, Hanel R, Combes M. An estimate of the PH_3, NH_3, CH_3D and GeH_4 abundances on jupiter from the voyager IRIS data at 4.5 μm. Icarus 1982;49:416–26.

[9] Chen F, Judge DL, Wu CYR, Caldwell J, White HP, Wagener R. High-resolution, low–temperature photoabsorption cross sections of C_2H_2, PH_3, AsH_3, and GeH_4, with application to saturn's atmosphere. J Geophys Res 1991;96:17519–27.

[10] Atreya SK, Mahaffy PR, Niemann HB, Wong MH, Owen TC. Composition and origin of the atmosphere of jupiter – an update, and implications for the extrasolar giant planets. Planet Space Sci 2003;51:105–12.

[11] Lodders K. Jupiter formed with more tar than ice. Astrophys J 2004;611:587–97.

[12] Asplund M, Grevesse N, Sauval J, Scott P. The chemical composition of the sun. Ann Rev Astron Astrophys 2009;47:451–522.

[13] Lodders K. Atmospheric chemistry of the gas giant planets; 2010. http://www.geochemsoc.org/publications/geochemicalnews/gn142jan10/atmosphericchemistryoftheg/.

[14] Agostini M, Allardt M, Andreotti E, Bakalyarov AM, Balata M, Barabanov I, et al. The background in the $0\nu\beta\beta$ experiment GERDA. Eur Phys J 2014;74:1–25.

[15] Haller EE. Germanium: from its discovery to sige devices. Mater Sci Semicond Process 2006;9:408–22.

[16] Kattenberg HW, Gabes W, Oskam A. Infrared and laser raman gas spectra of GeH_4. J Mol Spectrosc 1972;44:425–42.

[17] Ozier IO, Rosenberg A. The forbidden rotational spectrum of GeH_4 in the ground vibronic state. Can J Phys 1973;51(17):1882–95.

[18] Curl RF, Oka T, Smith DS. The observation of a pure rotational Q-branch transition of methane by infrared-radio frequency double resonance. J Mol Spectrosc 1973;46:518–20.

[19] Curl Jr R.F. Infrared-radio frequency double resonance observations of pure rotational Q-branch transitions of methane. 1973. 48:165–73.

[20] Kreiner WA, Oka T. Infrared - radio-frequency double resonance observations of $\Delta J = 0$ "forbidden" rotational transitions of SiH_4. Can J Phys 1975;53:2000–6.

[21] Kreiner WA, Andresen U, Oka T. Infrared-microwave double resonance spectroscopy of GeH_4. J Chem Phys 1977;66:4662–5.

[22] Kreiner WA, Orr BJ, Andresen U, Oka T. Measurement of the centrifugal-distortion dipole moment of GeH_4 using a CO_2 laser. Phys Rev A 1977;15:2298–304.

[23] Kagann RH, Ozier I, Gerry MCL. The centrifugal distortion dipole moment of silane. J Chem Phys 1976;64:3487–8.

[24] Lepage P, Brégier R, Saint-Loup R. La bande ν_3 du germane. C R Acad Sci Ser-B 1976;B283:179–80.

[25] Kagann RH, Ozier I, McRae GA, Gerry MCL. The distortion moment spectrum of GeH_4: the microwave Q branch. Can J Phys 1979;57:593–600.

[26] Fox K, Halsey GW, Daunt SJ, Kennedy RC. Transition moment for ν_3 of $^{74}GeH_4$. J Chem Phys 1979;70:5326–7.

[27] Kreiner WA, Magerl G, Furch B, Bonek E. IR laser sideband observations in GeH_4 and CD_4. J Chem Phys 1979;70:5016–20.

[28] Magerl G, Schupita W, Bonek E, Kreiner WA. Observation of the isotope effect in the ν_2 fundamental of germane. J Chem Phys 1980;72:395–8.

[29] Kreiner WA, Opferkuch R, Robiette AG. Turner PH. the ground–state rotational constants of germane. J Mol Spectrosc 1981;85:442–8.

[30] Lepage P, Champion JP, Robiette AG. Analysis of the ν_3 and ν_1 infrared bands of GeH_4. J Mol Spectrosc 1981;89:440–558.

[31] Schaeffer RD, Lovejoy RW. Absolute line strengths of $^{74}GeH_4$ near 5 μm. J Mol Spectrosc 1985;113:310–14.

[32] Zhu Q, Thrush BA, Robiette AG. Local mode rotational structure in the (3000) Ge-H stretching overtone ($3\nu_3$) of germane. Chem Phys Lett 1988;150:181–3.

[33] Zhu Q, Thrush BA. Rotational structure near the local mode limit in the (3000) band of germane. J Chem Phys 1990;92:2691–7.

[34] Campargue A, Vetterhöffer J, Chenevier M. Rotationally resolved overtone transitions of $^{70}GeH_4$ in the visible and near-infrared. Chem Phys Lett 1992;192:353–6.

[35] Zhu Q, Campargue A, Vetterhöffer J, Permogorov D, Stoeckel F. High resolution spectra of GeH_4 v = 6 and 7 stretch overtones. the perturbed local mode vibrational states. J Chem Phys 1993;99:2359–64.

[36] Sun F, Wang X, Liao J, Zhu Q. The (5000) local mode vibrational state of germane: a high-resolution spectroscopic study. J Mol Spectrosc 1997;184:12–21.

[37] Chen XY, Lin H, Wang XG, Deng K, Zhu QS. High-resolution fourier transform spectrum of the (4000) local mode overtone of GeH_4: local mode effect. J Mol Struct 2000(517–518):41–51.

[38] Boudon V, Grigoryan T, Philipot F, Richard C, Kwabia Tchana F, Manceron L, Rizopoulos A, Vander Auwera J, Th E. Line positions and intensities for the ν_3 band of 5 isotopologues of germane for planetary applications. J Quant Spectrosc Radiat Transf 2018;205:174–83.

[39] Corice Jr RJ, Fox K, Fletcher WH. Studies of absorption spectra of GeH_4 in the 2–17 μ region. J Mol Struct 1972;41:95–104.

[40] Daunt SJ, Halsey GW, Fox K, Lovell RJ, Gailar NM. High-resolution infrared spectra of ν_3 and $2\nu_3$ of germane. J Chem Phys 1978;68:1319–21.

[41] Zhu Q, Qian H, Thrush BA. Rotational analysis of the (2000) and (3000) bands and vibration-rotation interaction in germane local mode states. Chem Phys Lett 1991;186:436–40.

[42] Halonen L, Robiette AG. Rotational energy level structure in the local mode limit. J Chem Phys 1986;84:6861–71.

[43] Child MS, Zhu QS. Vibration–rotation hamiltonian of tetrahedral molecules in the local–mode model. Chem Phys Lett 1991;184:41–4.

[44] Zhu QS, Zhang BS, Ma YR, Qian HB. Local–mode rotational structure in the (3000) and (5000) stretching overtone bands of silane. Chem Phys Lett 1989;164:596–9.

[45] Zhu QS, Zhang BS, Ma YR, Qian HB. The (3000), (4000) and (5000) stretching overtone bands of silane – i. the effect of local–mode vibration on rotational constants. Spectrochim Acta 1990;46A:1217–22.

[46] Zhu QS, Ma H, Zhang BS, Ma YR, Qian HB. The (3000), (4000) and (5000) stretching overtone bands of silane – II. the rotational analysis in a normal—mode picture. Spectrochim Acta 1990;46A:1323–31.

[47] Gordon IE, Rothman LS, Hill C, Kochanov RV, Tan Y, Bernath PF, et al. The HITRAN 2016 molecular spectroscopic database. J Quant Spectrosc Radtat Transfer 2017;203:3–69.

[48] Hecht T. The vibration-rotation energies of tetrahedral XY_4 molecules. part I. Theory of spherical top molecules. J Mol Spectrosc 1960;5:355–89.

[49] Niederer HM. The infrared spectrum of methane. München: Verlag Dr. Hut; 2012.

[50] Niederer HM, Wang XG, Carrington T, Albert S, Bauerecker S, Boudon V, Quack M. Analysis of the rovibrational spectrum of $^{13}CH_4$ in the octad range. J Mol Spectrosc 2013;291:33–47.

[51] Sage ML, Jortner J. Bond modes. Adv Chem Phys 1981;47:293–322.

[52] Halonen L, Child MS. A local mode model for tetrahedral molecules. Mol Phys 1982;46:239–55.

[53] Halonen L, Child MS. Local mode theory for C_{3v} molecules: CH_3D, CHD_3, SiH_3D, and $SiHD_3$. J Chem Phys 1983;79:4355–62.

[54] Child MS, Halonen L. Overtone frequencies and intensities in the local mode picture. Adv Chem Phys 1984;57:1–58.

[55] Mills IM, Robiette AG. On the relationship of normal modes to ocal modes in molecular vibrations. Mol Phys 1985;56:743–65.

[56] Lukka T, Halonen L. Molecular vibrations and local modes. J Chem Phys 1994;101:8380–90.

[57] Ulenikov ON, Tolchenov RN, Zhu QS. "Expanded" local mode approach for $XY_2(c_{2v})$ molecules. Spectrochim Acta A 1996;52:1829–924.

[58] Fano U, Racah G. Irreducible tensorial sets. New York: Academic Press; 1959.

[59] Wigner EP. Quantum theory of angular momentum. New York: Academic Press; 1965.

[60] Varshalovitch DA, Moskalev AN, Khersonsky VK. Quantum theory of angular momentum. Nauka: Leningrad; 1975.

[61] Boudon V, Champion JP, Gabard T, Loëte M, Rotger M, Wenger C, Quack M. Spherical top theory and molecular spectra. In: Merkt F, editor. Handbook of high–resolution spectroscopy, vol.3. Wiley; 2011. p. 1437–60.

[62] Moret-Bailly J. Sur l'interprétation des spectres de vibration-rotation des molécules à symmétrie tétraédrique ou octaédrique. Cah Phys 1961;15:238–314.

[63] Champion JP, Pierre G, Michelot F, Moret-Bailly J. Composantes cubiques normales des tenseurs spheriques. Can J Phys 1977;55:512–20.

[64] Champion JP. Developpement complet de l'hamiltonien de vibration-rotation adapté à1'étude des interactions dans les molécules toupies sphériques. application aux bandes ν_2 et ν_4 de $^{12}CH_4$. Can J Phys 1977;55:1802–28.

[65] Boudon V, Champion JP, Gabard T, Loëte M, Michelot F, Pierre G, Rotger M, Wenger C, Rey M. Symmetry–adapted tensorial formalism to model rovibrational and rovibronic spectra of molecules pertaining to various point groups. J Mol Spectrosc 2004;228:620–34.

[66] Cheglokov AE, Ulenikov ON, Zhilyakov AS, Cherepanov VN, YuS M, Malikova AB. On the determination of spectroscopic constants as functions of intramolecular parameters. J Phys B 1989;22:997–1015.
[67] Nielsen HH. The vibration–rotation energies of molecules. Rev Mod Phys 1951;23:90–136.
[68] Watson JKG. Determination of centrifugal distortion coefficients of asymmetric–top molecules. J Chem Phys 1967;46:1935–49.
[69] Papousek D, Aliev MR. Molecular vibrational–rotational spectra. Amsterdam, Oxford, New York: Elsevier Scientific Publishing Company; 1982.
[70] Ulenikov ON, Bekhtereva ES, Albert S, Bauerecker S, Hollenstein H, Quack M. High–resolution near infrared spactroscopy and vibrational dynamics of dideuteromethane (CH_2D_2). J Phys Chem A 2009;113:2218–31.
[71] Ulenikov ON, Gromova OV, Bekhtereva ES, Belova AS, Bauerecker S, Maul C, Sydow C, Horneman VM. High resolution analysis of the (111) vibrational state of SO_2. J Quant Spectrosc Radiat Transfer 2014;144:1–10.
[72] Ulenikov ON, Onopenko GA, Bekhtereva ES, Petrova TM, Solodov AM, Solodov AA. High resolution study of the $\nu_5+\nu_{12}$ band of c_2h_4. Mol Phys 2010;108:637–47.
[73] Zhilinskii BI. Method of irreducible tensorial sets in molecular spectroscopy. Moscow: Moscow State University Press; 1981.
[74] Moret Bailly J, Gautier L, Montagutelli J. Clebsch–gordan coefficients adapted to cubic symmetry. J Mol Spectrosc 1965;15:355–77.
[75] Rey M, Boudon V, Ch W, Pierre G, Sartakhov B. Orientation of o(3) and $SU(2)\otimes C_i$ representation in cubic point groups (O_h, T_d) for application to molecular spectroscopy. J Mol Spectrosc 2003;219:313–25.
[76] Loéte M. Développement complet du moment dipolaire des molécules tétraédriques. application aux bandes triplement dégénérées et *à* la diade ν_2 et ν_4. Can J Phys 1983;61:1242–59.
[77] Saveliev VN, Ulenikov ON. Calculation of vibration–rotation line intensities of polyatomic molecules based on the formalism of irreducible tensorial sets. J Phys B 1987;20:67–83.
[78] Bykov AD, Makushkin Yu S, Ulenikov ON. On isotope effect in polyatomic molecules. some comments on the method. J Mol Spectrosc 1981;85:462–79.
[79] Halonen L. Stretching vibrational states in germane. J Phys Chem 1989;93:631–4.
[80] Wenger C, Boudon V, Champion JP, Pierre G. Highly–spherical top data system (HTDS) software for spectrum simulation of octahedral XY_6 molecules. J Quant Spectrosc Radiat Transfer 2000;66:1–16.